COMPUTER IMPLEMENTATION OF AN ELASTIC-PLASTIC CONCRETE RELATIONSHIP

D. W. MURRAY, L. CHITNUYANONDH, C. WONG

University of Alberta, Department of Civil Engineering, Edmonton, Alberta T6G 2G7, Canada

SUMMARY

The purpose of this paper is to describe the difficulties that arose, and the strategies that were developed to overcome these difficulties, during the incorporation of a relatively complex elastic-plastic concrete constitutive relationship into an existing computer code for the analysis of axisymmetric loading acting on thin shells of revolution. The program had the capability of elastic-plastic analysis using a von-Mises yield curve prior to any modification by the writers.

The paper reviews the formulation of the parent program and of the constitutive relationship. The overall solution procedure is then discussed. The techniques of determining the incremental material quantities by a subincremental procedure are presented with reference to appropriate flow charts. Specific problems dealt with are: (a) the method of treating a yield function which has different analytical expression in different regions of biaxial stress space; (b) the problem of avoiding false roots of the yield function; (c) the problem of developing criteria to determine the effective size of strain subincrement when abrupt changes occur in material properties within a strain increment; (d) the technique of assuring convergence of the subincremental procedure; (e) correcting for drift of the stress point off the yield curve; and (f) the problem of efficiently finding the root of the complex yield function. While many of these problems have been previously addressed, it is hoped that the experience of the writers will prove beneficial to others working in the area.

References are cited to the application of the technique to significant problems in the prediction of the overload behavior of the thin-walled prestressed concrete secondary containment structures.

1. Introduction

Many structural programs now exist for the solution of elastic-plastic problems. One should be able to adapt a program based on a flow theory of plasticity to a variety of different materials by modifying the flow rule, the hardening rule and the yield function.

It is usual to analyse thin-walled prestressed concrete secondary containment structures by using a "tension cut-off" analysis. However, unless one attempts to locate and identify individual cracks, such an analysis overestimates the deformation associated with cracking behavior. For this reason it is useful to associate a stiffness with cracked concrete.

The writers have participated in the development of an elastic-plastic material simulation for concrete response in which the effect of cracking is reflected by a degrading stress-strain curve [1,2]. It has been shown that such a material simulation can produce results which correlate well with experimental tests of prestressed concrete wall segments [1,3,4] and also with measured post-cracking response of more complex structures [5,6].

The structures analyzed with the aforementioned constitutive relationship have been thin shell type structures which may be considered to be representative of prestressed concrete secondary containment structures. The computer code into which the constitutive relationship was incorporated for the purpose of carrying out the foregoing analyses was the BOSOR5 code [7,8]. Since this program was operational with a 'metal' flow theory of plasticity, and was capable of carrying out elastic-plastic analyses of layered segmented shells in which a different material relationship could be assigned to each layer, it was an ideal vehicle in which to incorporate the new plasticity theory.

While there was no difficulty in principle in incorporating the new constitutive theory into the BOSOR5 code, a number of practical difficulties arose. The object of this paper is to identify these problems and describe the strategies the writers used in coping with them. Although many investigators have undoubtedly overcome similar problems, it is hoped that the experience of the writers will prove beneficial to those working in the area who have not yet encountered them. In order to place these in their proper context it is first necessary to review the governing equations, the form of the constitutive equations and the solution technique.

2. Governing Equations

The derivation of the governing equations is described in detail in Refs. 8, 9 and 10. For an axisymmetric shell of revolution subjected to axisymmetric loading the Newton-Raphon equations may be written as

$$\Big[\int_{\ell} \Big(\langle \frac{\partial \kappa}{\partial q_i} \rangle [\tilde{C}] \{ \frac{\partial \kappa}{\partial q_j} \} + \langle \langle \kappa \rangle [\tilde{C}]^T + \langle N^* \rangle \rangle \{ \frac{\partial^2 \kappa}{\partial q_i \partial q_j} \} \Big) ds$$

$$- \frac{\partial^2 W}{\partial q_i \partial q_j} \Big] \Delta q_j = \frac{\partial W}{\partial q_i} - \int_{\ell} \Big(\langle \langle \kappa \rangle [\bar{C}]^T + \langle N^* \rangle \rangle \{ \frac{\partial \kappa}{\partial q_i} \} \Big) ds \qquad (1)$$

in which Δq_j represents increments of the displacement coordinate q_j. The indeces i and j have a range of 1 to N where N is the total number of degress of freedom of the system. The vector $\{\kappa\}$ is the vector of reference surface deformations defined as

$$\langle \kappa \rangle = \langle \varepsilon_1 \ \varepsilon_2 \ \kappa_1 \kappa_2 \rangle \tag{2}$$

in which ε_1 and ε_2 are the reference surface strains and κ_1 and κ_2 are thereference surface curvatures in the meridional and circumferential directions as indicated by 1 and 2, respectively. The matrix $[\tilde{C}]$ represents the tangent stiffness associated with increments of midsurface deformations and arises after integration of the material tangent stiffness matrix, $[D_{EP}]$, through the thickness. It is defined as

$$[\tilde{C}] = 2\pi r_o \int_t [Z]^T [D_{EP}][Z] \frac{r}{r_o}(1 + z/R_1)(1 + z/R_2)dz \tag{3}$$

in which z is a thickness coordinate, t is the shell thickness, r is the radius normal to the axis of symmetry, r_o is the value of r on the reference surface, R_1 and R_2 are the meridional and normal circumferential radii of curvature, and [Z] is the product matrix arising from the Love-Kirchhoff assumptions in the equation

$$\{\varepsilon\} = \begin{bmatrix} (1 + z/R_1)^{-1} & \cdot \\ \cdot & (1 + z/R_2)^{-1} \end{bmatrix} \begin{bmatrix} 1 & \cdot & -z & \cdot \\ \cdot & 1 & \cdot & -z \end{bmatrix} \{\kappa\} \tag{4}$$

where $\{\varepsilon\}$ is the vector of principal strains at a distance of z from the reference surface.

The vector $\{N^*\}$ of eq. 1 is the vector of equivalent thermal forces, defined as

$$\{N^*\} = 2\pi r_o \int_t [Z]^T \{\sigma^*\} \frac{r}{r_o}(1 + z/R_1)(1 + z/R_2)dz \tag{5}$$

in which $\{\sigma^*\}$ is the vector of equivalent thermal strains defined as

$$\{\sigma^*\} = [D]\{[C]\{\varepsilon\} - \{\varepsilon^P\} - \{\varepsilon^c\} - \{\varepsilon^T\}\} \tag{6}$$

in which [D] is the initial linear elastic constitutive matrix; $\{\varepsilon\}$, $\{\varepsilon^P\}$, $\{\varepsilon^c\}$ and $\{\varepsilon^T\}$ are the vectors of total, plastic, creep and thermal strains, respectively; and [C] is the matrix arising from the plasticity theory which defines the increments of plastic strain in terms of the increments in total strain through the equation

$$\{\Delta\varepsilon^P\} = [C]\{\Delta\varepsilon\}. \tag{7}$$

Assuming $\{\varepsilon^c\}$ and $\{\varepsilon^T\}$ are specified independently of stress increments, the time-independent stress increment $\{\Delta\sigma\}$ may be written as

$$\{\Delta\sigma\} = [D]\{\{\Delta\varepsilon\} - \{\Delta\varepsilon^P\}\} \tag{8}$$

which may be written as

$$\{\Delta\sigma\} = [D_{EP}]\{\Delta\varepsilon\} \tag{9}$$

where eq. 7 now permits the derivation of $[D_{EP}]$ as

$$[D_{EP}] = [D][I - C] \tag{10}$$

To complete the definition of the quantities appearing in eq. 1 it is necessary to note that W represents the work of the external forces, s represents a length coordinate along the meridian and ℓ represents the length of the meridian.

Eq. 1 may be written symbolically as

$$[K_T([\tilde{C}],\ \{N^*\},\kappa)]\{\Delta q\} = \{Q[\tilde{C}],\{N^*\},\ \kappa)\} \tag{11}$$

in which the matrix $[K_T]$ denotes the tangent stiffness matrix and $\{Q\}$ denotes the unbalanced load vector. The notation emphasizes the nonlinear variables upon which both of these matrices depend. Both the section stiffness matrices $[\tilde{C}]$ and the equivalent thermal force vector $\{N^*\}$ are dependent on the $[C]$ matrix of eq. 7 and attention is now directed to this aspect of the formulation.

3. The Concrete Constitutive Relationship

The concrete constitutive relationship has been described in detail in Refs. 1, 2 and 10. The yield function may be expressed as

$$F(\sigma_1,\ \sigma_2,\ \sigma_c,\ \sigma_{t1},\ \sigma_{t2}) = 0 \tag{12}$$

in which $(\sigma_1,\ \sigma_2)$ represents a point in biaxial stress space at incipient yield; and σ_c, σ_{t1} and σ_{t2} are the current yield strengths in compression and in tension in directions 1 and 2, respectively. The form of the yield function adopted for this study is rather complex, having different analytical expressions in different zones of biaxial stress space. It is illustrated schematically in Fig. 1 and summarized algebraically in Table 1.

The three yield strengths σ_c, σ_{t1} and σ_{t2} are assumed to depend on the three plastic strain parameters λ, μ_1, and μ_2, respectively. These plastic strain parameters are accumulated from increments in the equivalent plastic strain, $\bar{\varepsilon}^P$. The rate of change of these parameters has been expressed in terms of the equivalent plastic strain rate as

$$\dot{\lambda} = \alpha\dot{\bar{\varepsilon}}^P \tag{13a}$$

$$\dot{\mu}_1 = \beta_1\dot{\bar{\varepsilon}}^P \tag{13b}$$

$$\dot{\mu}_2 = \beta_2\dot{\bar{\varepsilon}}^P \tag{13c}$$

in which

$$\dot{\bar{\varepsilon}}^P = \sqrt{\langle\dot{\varepsilon}^P\rangle\{\dot{\varepsilon}^P\}} \tag{13d}$$

and $\cdot$ indicates a time derivative. The decomposition parameters α, β_1 and β_2 have been taken as indicated in Table 1 and satisfy the constraint that

$$\alpha + \beta_1 + \beta_2 = 1. \tag{13e}$$

The rate of plastic straining is assumed to follow the normality rule. That is

$$\{\dot{\varepsilon}^P\} = \{B\}\ \dot{\varepsilon}^P/B \tag{14a}$$

in which

$$\langle B\rangle = \langle\frac{\partial F}{\partial\sigma_1},\ \frac{\partial F}{\partial\sigma_2}\rangle \tag{14b}$$

and B is the magnitude of <B>.

Finally it is assumed that yield strengths σ_c, σ_{t1}, and σ_{t2} may be related to the uniaxial response through the strain parameters λ, μ_1, and μ_2 by the relations

$$\sigma_c = \sigma_c^0 + g(\lambda) \tag{15a}$$

$$\sigma_{t1} = \sigma_t^0 + h(\mu_1) \tag{15b}$$

$$\sigma_{t2} = \sigma_t^0 + h(\mu_2) \tag{15c}$$

where σ_t^0 and σ_c^0 are initial yield values in tension and compression, respectively, and the functions g and h are hardening functions defined by the uniaxial stress-strain curves.

The incremental plastic strain matrix [C] of eq. 7 may now be derived from the condition

$$\dot{F} = 0 \tag{16}$$

by the normal procedure [1, 2, 10, 11] as

$$[C] = \{B\}\langle B\rangle[D]/A \tag{17a}$$

in which

$$A = \langle B\rangle[D]\{B\} - B\Big(\alpha g'(\lambda)\partial F/\partial\sigma_c + \beta_1 h'(\mu_1)\partial F/\partial\sigma_{t1} + \beta_2 h'(\mu_2)\partial F/\partial\sigma_{t2}\Big) \tag{17b}$$

where ' indicates differentiation with respect to the argument. The tangent matrix of eq. 10, and the effective stress vector of eq. 6, and consequently all material and stress dependent quantities of eq. 1, may now be evaluated.

4. The Solution Procedure

The static solution procedure of the BOSOR5 code [7] is outlined in the flow chart of Fig. 2. The Newton-Raphson solution is carried out in two nested iterative loops. The strain displacement equations are nonlinear. Hence the midsurface strains, $\{\kappa\}$, are nonlinear functions of the nodal displacements $\{q\}$. The inner loop iterates on this nonlinear geometry while the matrices $[\tilde{C}]$, and the equivalent thermal load vectors $\{N^*\}$, are held constant. Upon convergence of the inner loop, the plastic strains, effective thermal stresses and incremental material stiffness matrices are re-evaluated using a "subincrement procedure" [7,8] and then new values are obtained for $[\tilde{C}]$ and $\{N^*\}$. The essential idea in the subincrement procedure is to divide the total strain increment for the load step into a set of small subincrements which accumulate to the total strain increment, and to evaluate the incremental quantities for each subincrement. In this way the flow of the material can be followed closely. The entire procedure is then repeated in a new pass through the outer loop until the displacements repeat in two successive passes.

A flow chart for the subincrement procedure, indicated by box (a) in Fig. 2., is shown in Fig. 3. This procedure follows closely the procedure of Bushnell [7,8] but contains a number of modifications required for processing the more complex yield function expressed in Table 1. We now address the problems that arose in the implementation of the constitutive relationship with reference to the FLOW3 subroutine shown in Fig. 3. Creep strains and thermal strains are not included in the present discussion.

5. Details of Implementation

The first decision to be made in the FLOW 3 subroutine (Fig. 3) is to determine if the strain increment produces 'loading' or 'unloading' of the yield function. This is done by computing the elastic stress change $\{\Delta\sigma^E\}$ using the linear elastic constitutive matrix. Thus

$$\{\sigma^E\} = [D]\{\Delta\varepsilon\} \tag{18}$$

Augmenting the stress at the previously converged point, $\{\sigma\}_0$, by this vector produces the stress at the end of the strain increment, providing the stress change is elastic. A number of possibilities now arise, as illustrated in Fig. 4. (In Fig. 4 the initial stress point is indicated by a subscript 1 and the augmented stress point is indicated by the subscript 2, for various cases designated by A to E). For cases A and B, which remain entirely within the yield curve, the augmented stress point provides the correct stresses since no 'loading' occurs. This is detected by the condition

$$F(\{\sigma\}_0 + \{\Delta\sigma^E\}, \sigma_c, \sigma_{t1}, \sigma_{t2}) < 0. \tag{19}$$

Thus, when eq. 19 is satisfied no plastic straining occurs and the subroutine follows Path 1 as indicated.

If the test of eq. 19 fails, loading occurs and plastic strains and incremented properties must be computed. In this case the location of the initial stress point $\{\sigma\}_0$ relative to the yield function is determined. If

$$F(\{\sigma\}_0, \sigma_c, \sigma_{t1}, \sigma_{t2}) > 0 \tag{20}$$

the initial stress point is outside the yield curve. In this case a normal subincrement procedure is initiated as indicated by Path 3 of Fig. 3. If the test of eq. 20 fails the initial stress point lies on or within the yield curve and a condition such as C, D, or E of Fig. 4 has been detected. In this case the fraction, μ, of the strain increment to bring the stress point to the yield curve is computed, by finding μ as a root of the equation

$$F(\{\sigma\}_0 + \mu\{\Delta\sigma^E\}, \sigma_c, \sigma_{t1}, \sigma_{t2}) = 0 \tag{21}$$

It has been the writers' experience that in order to avoid difficulties during execution it is necessary to anticipate that the stress change $\{\Delta\sigma^E\}$ may be arbitrary in both magnitude and direction. Indeed it may be several times the maximum dimension of the yield surface. Thus the stress point $\{\sigma\} + \{\Delta\sigma^E\}$ may be several zones removed from the initial stress point. Two difficulties arise in the above procedure. When the yield function is complex the test of eq. 19 may be unreliable since there may be a number of zones other than that within the yield curve for which $F < 0$. There may also be zones within the yield curve for which $F > 0$. Furthermore, it is necessary to be able to determine the root of eq. 21 in an efficient manner and avoid false roots associated with undesired sign changes.

The writers found that these problems could be eliminated by defining a simple region bounded on the outside by a simple curve circumscribing the yield curve and bounded on the inside by a simple curve inscribing the yield curve. Such a simple region is illustrated in Fig. 5. The proper sign of F for points not falling within this region can be simply assigned and, providing the sign for each function is correct within its restricted zone of the simple region, no difficulties occur with the tests of eqs. 19 and 20.

In order to eliminate the problem of false roots in the solution of eq. 21 the points of intersection of the stress path from $\{\sigma\}_0$ to $\{\sigma\}_0 + \{\Delta\sigma^E\}$ with the boundaries of the simple region are first determined. The search for the root is then confined to points along the line within the region. Since the location of the root is known within narrow limits the method of bisection is simple, reliable and efficient for its determination.

To detect points such as E of Fig. 4, the scalar product of $\{\Delta\sigma^E\}$ and the normal to the yield function, denoted as DOT, is evaluated. If DOT < 0 and the test of eq. 19 fails a root is determined by stepping back from point E2.

The portion of the strain increment associated with plastic straining for the variety of stress increments illustrated in Fig. 4 has now been determined. It remains to divide this portion into subincrements and successively impose the subincremental strains until they accumulate to the required values. A fundamental question is: "How small must the subincrements be?" The writers were unable to determine any rigorous method of answering this question. However it was apparent that for numerical efficiency the size of subincrement should vary depending on the zone in which plastic straining occured and the rate of softening of the material.

The material model relates the incremental quantities to the uniaxial stress-strain curves. These curves were approximated as piecewise linear [1,2,3,4]. A 'break' in the slope of a piecewise linear stress-strain curve occurs at the junction of two linear segments of the curve and this results in an abrupt discontinuity of the incremental stiffness as the material strains through this point. Thus, the values of g' and h' in eq. 17b are piecewise constant.

The basic number of subincrements, called NOSUB in Fig. 3, was determined by subroutine SUBDIV. The following three criteria were used to determine the maximum size of subincrement. (a) $\{\Delta\sigma\}$ as computed from the matrix $[D_{EP}]$ was limited to a fraction of the dimension of the yield curve. The fraction varied between 1 and 1/4 depending on the orientation of the stress change with respect to the yield curve. (b) The amount by which each yield strength changed was limited to 0.1 of its current value. (c) The strain in each direction was limited to a multiple of the initial yield strain. A multiple of 2 for tension and 1/2 for compression was used. The largest number of subincrements determined by these three criteria, denoted as NOSUB, was used for the analysis.

Subincrements of the size determined above were then sequentially applied. However, if within any subincrement a 'break' on a stress strain curve or a corner of the yield function was encountered, only the portion of the subincrement required to reach this point was applied. Since material properties change abruptly at these points a new control size for the subincrement (i.e. a new NOSUB) was then determined prior to continuing with the subincremental straining. Since the stress point drifts somewhat from the (moving) yield curve during a subincrement, a correction to the stress point was made at the end of each subincrement by a subroutine called DRIFT. DRIFT simply finds a root of the yield function on the line between the current stress point and the origin.

The subincrement procedure was then repeated with the number of subincrements increased to i times NOSUB at each stage, where i is the number of the pass through the subincrement process, until the change in the stress point between two successive passes was negligible.

The accumulated values of plastic strains and the updated values of $\{\sigma\}$, λ, μ_1, μ_2, $[C]$ and $[D_{EP}]$ are now consistent with the total strain for the given configuration, and the operations contained in box (a) of Fig. 2 have been completed.

6. Summary and Conclusions

A review of the three-parameter elastic-plastic constitutive theory for concrete and the equations for its implementation has been given. Some of the difficulties encountered in the implementation of this constitutive relationship and the strategies for overcoming these problems have been discussed. Applications of the current theory may be found in Refs. 1, 2 and 5.

7. Acknowledgements

This work was sponsored by the Atomic Energy Control Board of Canada, Ottawa, Canada, K1P 5S9.

References

/1/ Murray, D.W., Chitnuyanondh, L., Wong, C., and Rijub-Agha, K.Y., "Inelastic Analysis of Prestressed Concrete Secondary Containments:, Structural Engineering Report No. 67, Department of Civil Engineering, University of Alberta, Edmonton, Canada, T6G 2G7, July 1978.

/2/ Murray, D.W., Chitnuyanondh, L., Rijub-Agah, K.Y., and Wong, C., "A Concrete Plasticity Theory for Biaxial Stress Analysis", submitted to the Journal of the Engineering Mechanics Division, ASCE, August 1978.

/3/ Chitnuyanondh, L., Rizkalla, S., Murray, D.W., and MacGregor, J.G., "An Effective Uniaxial Tensile Stress-Strain Relationship for Prestressed Concrete", Structural Engineering Report No. 74, Department of Civil Engineering, University of Alberta, Edmonton, Canada, T6G 2G7, February 1979.

/4/ Chitnuyanondh, L., Rizkalla, S., Murray, D.W., and MacGregor, J.G., "Effective Tensile Stiffening in Prestressed Concrete Wall Segments", Transactions of SMiRT5 Paper No. J 3/4, Berlin, August 1979.

/5/ Rizkalla, S., Simmonds, S.H., and MacGregor, J.G., "A Test of a Model of a Thin-Walled Prestressed Concrete Secondary Containment Structure", Transactions of SMiRT5, Paper No. J 4/2, Berlin, August 1979.

/6/ Murray, D.W., Chitnuyanondh, L., and Wong, C., "Modelling and Predicting Behavior of Prestressed Concrete Secondary Containment Structures Using BOSOR5", Transactions of SMiRT5, Paper No. J 3/5, Berlin, August 1979.

/7/ Bushnell, D., "BOSOR5 - A Computer Program for Buckling of Elastic Plastic Complex Shells of Revolution Including Large Deflections and Creep",
(a) Vol. 1: User's Manual, Input Data", LMSC D407166, December 1974.
(b) Vol. 3: Theory and Comparisons with Tests", LMSC D407168, December 1974.
Lockheed Missiles and Space Company, Sunnyvale, Calif.

/8/ Bushnell, D., "A Strategy for the Solution of Problems Involving Large Deflection, Plasticity and Creep", International Journal for Numerical Methods in Engineering, Vol. 11, 1977, pp. 683-708.

/9/ Bushnell, D., "Stress, Stability and Vibration of Complex Branched Shells of Revolution: User's Manual for BOSOR4", LMSC D243605, Lockheed Missiles and Space Company, Sunnyvale, Calif.

/10/ Murray, D.W., Chitnuyanondh, L., and Wong, C., "Implementation of an Elastic-Plastic Concrete Relationship", submitted to Computer Methods in Applied Mechanics and Engineering, North Holland Publishing Company, February 1979.

/11/ Marcal, P.V., "Finite Element Analysis with Material Nonlinearities - Theory and Practice", Recent Advances in Matrix Methods of Structural Analysis and Design, University of Alabama Press, 1971, pp. 257-282.

Table 1 Definition of Yield Function and Parameters

Zone	Function F	Range of		Decomposition Parameters		
		σ_1/σ_2	σ_2/σ_c	α	β_1	β_2
1	$\sigma_{t1}\sigma_{t2} \cdot f_1(\sigma_1/\sigma_{t1}, \sigma_2/\sigma_{t2})$	≥ 0	≥ 0	0	$(B_1/B)^2$	$(B_2/B)^2$
2	$\sigma_2 + \sigma_{t2} \cdot f_2(\sigma_1/\sigma_c)$	$[-\sigma_2/2\sigma_{t2}, 0]$	> 0	$-\sigma_1/\sigma_c$	0	$1 - \alpha$
3	$\sigma_2 + \sigma_{t2} \cdot f_3(\sigma_1/\sigma_c)$	$<-\sigma_2/2\sigma_{t2}$	> 0	$-\sigma_1/\sigma_c$	0	$1 - \alpha$
4	$\sigma_c \cdot f_4(\sigma_2/\sigma_c) - \sigma_1$	$<k\sigma_2/\sigma_c$	≤ 0	1	0	0
5	$\sigma_c \cdot f_5(\sigma_1/\sigma_c, \sigma_2/\sigma_c) - \sigma_c$	$[k\sigma_2/\sigma_c, \sigma_2/k\sigma_c]$	≤ 0	1	0	0
6	$\sigma_c \cdot f_4(\sigma_1/\sigma_c) - \sigma_2$	$(\sigma_2/k\sigma_c, 0)$	≥ 0	1	0	0
7	$\sigma_1 + \sigma_{t1} \cdot f_3(\sigma_2/\sigma_c)$	> 0	$<-\sigma_1/2\sigma_{t1}$	$-\sigma_2/\sigma_c$	$1 - \alpha$	0
8	$\sigma_1 + \sigma_{t1} \cdot f_2(\sigma_2/\sigma_c)$	> 0	$[-\sigma_1/2\sigma_{t1}, 0]$	$-\sigma_2/\sigma_c$	$1 - \alpha$	0

Notation: $k = 1.5849098$ $\qquad f_4(x) = 0.6314307x^3 + 1.4615073x^2 + 1.1x - 1$

$f_2(x) = 0.4\,x^2 - 1$ $\qquad f_5(x_1, x_2) = [x_1^2 + x_2^2 - 1.23\,x_1x_2]^{1/2}$

$f_3(x) = 2.8x^2 + 2.4x - 0.4$

$$f_1(x_1, x_2) = 0.01 - \frac{(1 - 0.99\,x_1 + a\,x_1x_2)\,(1 - 0.99\,x_2 + a\,x_1x_2)}{(1 - 0.0001\,x_1x_2)^2}, \text{ where } a = 0.0098$$

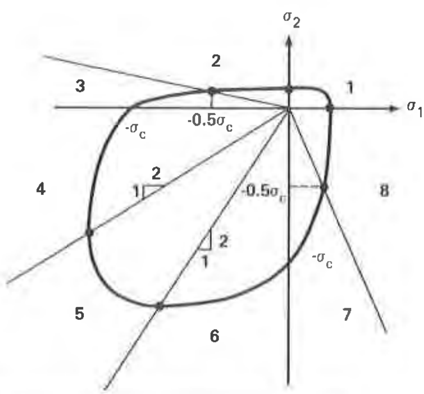

Zone	Type of Curve*
1	Modified Hyperbola
2, 3, 7, 8	Quadratic Splines
4, 6	Cubic Splines
5	Modified Ellipse

● Indicates Point of Tangency
* Analytical Expressions in Table 1
9 Zone Number
—— Divisions Between Zones

Figure 1 Zones of Yield Function

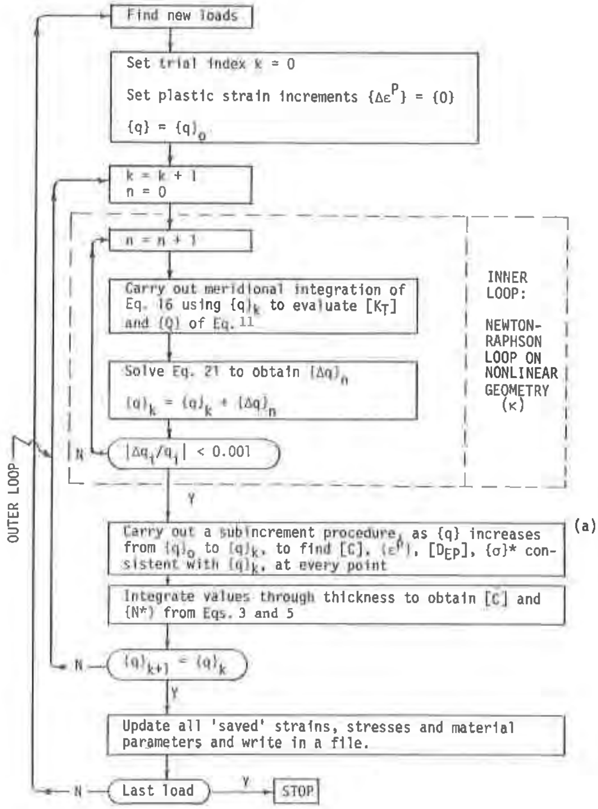

Figure 2 Flow Chart of BOSOR5 Solution Technique

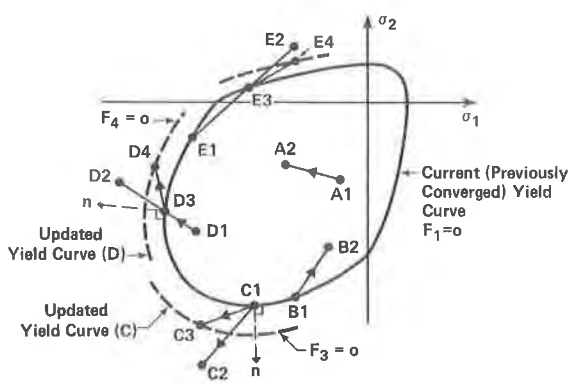

Figure 4 Points in Stress Space for Possible Strain Increments

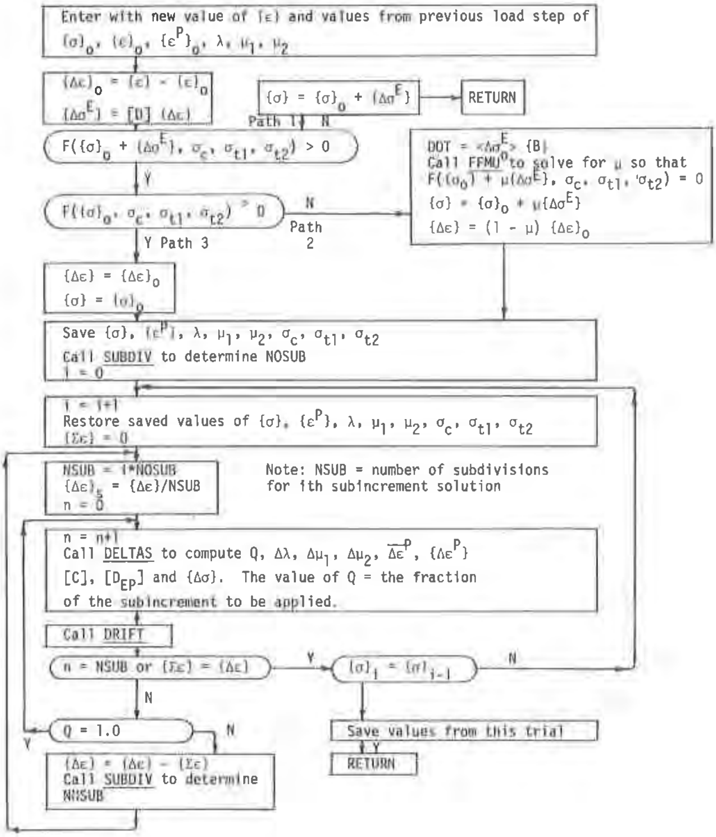

Figure 3 Flow Chart of FLOW3

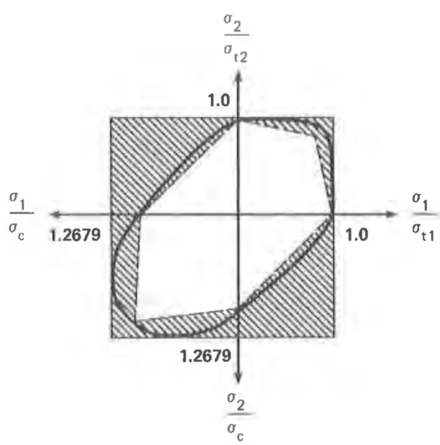

Figure 5 Bounded Region Containing Yield Curve